2020 17th International Conference on Electrical Engineering, Computing Science and Automatic Control (CCE)
Mexico City, Mexico. November 11-13, 2020

# A Fractal Octagonal-Shaped Transparent Antenna for C-band Applications

Fernando Lopez-Marcos
*Faculty of Electronic Science*
*Benemerita Universidad*
*Autonoma de Puebla, Mexico*
Puebla, Mexico
fernando.lopezmarcos@correo.buap.mx

Richard Torrealba-Melendez
*Faculty of Electronic Science*
*Benemerita Universidad*
*Autonoma de Puebla, Mexico*
Puebla, Mexico
richard.rorrrealba@correo.buap.mx

Marco Antonio Vasquez-Agustin
*Faculty of Electronic Science*
*Benemerita Universidad*
*Autonoma de Puebla, Mexico*
Puebla, Mexico
mava.vasquez@gmail.com

Jesus Manuel Muñoz-Pacheco
*Faculty of Electronic Science*
*Benemerita Universidad*
*Autonoma de Puebla, Mexico*
Puebla, Mexico
jesusm.pacheco@correo.buap.mx

Edna Iliana Tamariz-Flores
*Faculty of Computer Science*
*Benemerita Universidad*
*Autonoma de Puebla, Mexico*
Puebla, Mexico
iliana.tamariz@gmail.com

***Abstract*—. This work describes the analysis, design, and fabrication of a transparent planar antenna for C-band applications. The bandwidth of the antenna, according to measurements of the reflection coefficient $S_{11}$, is 3-6 GHz, with a peak value of -26 dB. The measured radiation pattern for the antenna is omnidirectional, with an average gain of -6.9 dB.**

***Keywords— transparent antenna, ultra-wideband, ITO, Minkowsky fractal, octagonal patch, CPW.***

## I. INTRODUCTION

The wireless communication systems have evolved rapidly in the last years. The requirements of the new technologies point to the optimized use of the electromagnetic spectrum. There are different alternatives to get better exploitation of different bands in the electromagnetic spectrum.

The C-band is one of the most used band because of the high data capacity and the links that do not require line of sight (LoS). The principal uses of the C-band are satellite communications, ISM applications. Although there are different assigned frequency bands in UHF, C-band, and K-band, the C-band is that offers the best relation between bandwidth and NLoS (no line of sight) links in 5G band mobile telephony systems [1]–[6].

The different frequencies of the C-band point to use a wideband to approach. The wideband antennas not only can be used to communication systems but also are used in applications of radiofrequency energy harvesting. The massive use of the C-band for commercial communications systems increases the energy to be harvested in comparison with other bands [7], [8].

There is recent work related to the application of transparent conductive films to design transparent antennas. The fabrication of transparent antennas consists of the integration of a transparent conductive film over a transparent dielectric substrate [9]–[13]. The main objective of fabricating transparent antennas is to make an easily integrable antenna in a wide variety of scenarios, which include glasses for vehicles [14], implementation of discrete base-stations (BS), the connectivity of solar panels, and others.

There is a variety of literature that reports the results of transparent antennas. Hakimi *et al.* [9] present a CPW-fed transparent antenna that consists of a ring resonator and a reduced-size ground plane. They used conductive material is ITO, reinforced with a gold layer to increase the conductivity of the plate. The antenna has a wideband behavior, which operates in the frequencies between 2-20 GHz, with a peak reflection coefficient of -20 dB in 7 GHz. Awalludin *et al*. [10] show the simulation of a square patch transparent antenna that operates at the 2.4 GHz Industrial, Scientific, and Medic (ISM) band. The antenna is fabricated with AZO conductive film, with tests of glass and quartz substrates. The obtained reflection coefficient $S_{11}$ of the antenna is -16 dB.

Other works make an effort to get optimization in the behavior of the antenna. Song *et al.* [11] propose a method to improve the properties of an antenna by increasing the conductivity of an $AgHT_4$ film with the addition of metallic particles in the borders of the antenna. The implemented antenna reaches a -15 dB of the reflection coefficient at the frequency of 2.4 GHz. Another example of the optimization of the design is the work of Li *et al*. [12] that consists of a transparent antenna made of Micro Metal Mesh Conductive (MMMC) film. The operation frequencies are 2.4 and 5.8 GHz, with a peak reflection coefficient of -22 dB. Finally, Eltresy *et al*. propose the design of a transparent multiband antenna that operates in both 2.4 and 3.7 GHz frequencies. They used conductive film is $AgHT_4$ over a plexiglass substrate.

This work describes the analysis, design, and fabrication of a transparent planar antenna for every frequency contained in C-band. The design consists of a planar monopole octagonal patch antenna, which is expected that have a wideband behavior. The antenna was fabricated with a 1 mm glass substrate with a 150 nm ITO (Indium-Tin Oxide) transparent conductive film. The feedline of the antenna was designed using a CPW (Coplanar Waveguide) with a separation of 0.3 mm between the feedline and the ground plane. The designed octagonal patch was modified with a Minkowsky-Like fractal structure. The objective of including fractals in the design is to test the

978-1-7281-8987-1/20/$31.00 ©2020 IEEE

improvement of the reflection coefficient and the increase of the electrical length without a significant increase in the physical length.

## II. Design

### A. Initial design

The design points to make a reduced size transparent antenna in order to integrate in a mobile system. In order to use a single-metallization substrate, the main antenna design consists of a coplanar waveguide (CPW) line that feeds an octagonal patch. This design has a wide band behavior [15]–[17]. The considered CPW model must include the particular features of the ITO film, which has lower conductivity in comparison with a metallic film (about three magnitude orders) and is thinner than the metallic film [18].

The selected design frequency for the antenna elements is 4 GHz, which is expanded due to the nature of the design. A 50 Ω impedance was considered for the design. This impedance was selected in the CPW feedline, considering a 0.3 mm of separation between the line and the ground plane. The analysis of the CPW feedline was made using the model described by Simmons [19], with the respective considerations studied by Shu *et al.* [20], related to the impact of the low-conductivity film in the dimensions of the CPW. The impedance $Z_0$ of the CPW is calculated using (1):

$$Z_0 = \frac{30\pi}{\sqrt{\varepsilon_{eff,t}}} \frac{K(k'_1)}{K(k_1)} \tag{1}$$

Where the parameter $\varepsilon_{eff,t}$ is the effective dielectric permittivity due to the substrate thickness and the separation between the line and the ground plane, meanwhile the function $K$ refers to the capacitance per unit length formed between the line and the ground plane. This parameter is evaluated through an approximation of the quotient $K(k)/K'(k)$, as shown in (2):

$$\frac{K(k)}{K'(k)} = \begin{cases} \dfrac{\pi}{\ln\left(2\left(\dfrac{1+\sqrt{k'}}{1-\sqrt{k'}}\right)\right)}, 0 \le k \le \dfrac{1}{\sqrt{2}} \\ \dfrac{\ln\left(2\left(\dfrac{1+\sqrt{k'}}{1-\sqrt{k'}}\right)\right)}{\pi}, \dfrac{1}{\sqrt{2}} \le k \le 1 \end{cases} \tag{2}$$

The initial frequency ($f$) for the octagonal patch design is described by (3) [7], [21], [22]:

$$f = \frac{7.2}{(l + r + p)k} \tag{3}$$

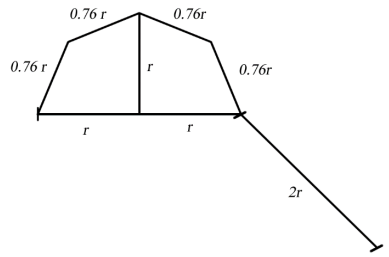


Fig. 1. Illustration of the structure that is replicated to get the fractal, where $r$ is radius of the octagon

In (3), the measure $l$ represents the patch diameter; meanwhile, $r$ represents the relative effective length due to the width of the patch, and $p$ represents the length of the transmission line, respectively. $k$ represents the effective length, which is calculated with the quotient of the patch diameter ($l$) and $2\pi$. For the case of an octagonal patch, the lateral diameter has the same length that the main diameter. Then, this patch is modeled with the parameters of a circular patch.

### B. Fractal geometry modification

It is proposed a fractal geometry modification to improve the performance of the antenna. The fractal geometry includes segments or structures that are repeated with determined scale rates. The objectives of using fractal structures are the increasing of the electrical length without a significant rise in the physical length. Other goals of the application of fractal structures are the modification of the reflection coefficient to get a concentrated narrowband or multiband antenna.

A Minkowsky fractal structure was proposed to increase the electrical length of the antenna. According to Vivek *et al* [21], the fractal dimension of the antenna is calculated with (4):

$$D = \frac{\log(N)^n}{\log(s)} \tag{4}$$

In (4), the number of segments of the geometry is defined by $N$, the number of parts in which every segment is divided with each iteration is $s$; finally, $n$ is the number of total iterations. Meanwhile, the initial length of the segment is defined by (5):

$$h = \left(\frac{N}{s}\right)^n \tag{5}$$

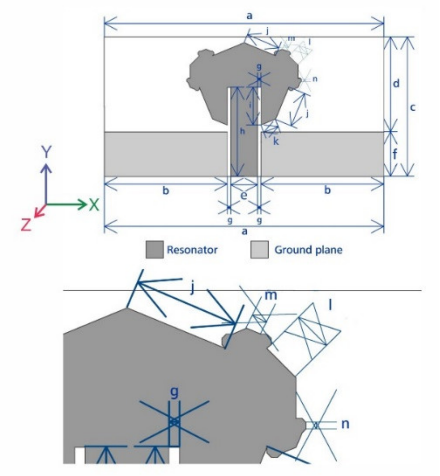


Fig. 2. Proposed antenna design.

TABLE I. ANTENNA DIMENSIONS

| Label | Dimension (mm) | Label | Dimension (mm) |
|---|---|---|---|
| a | 25 | h | 8 |
| b | 11 | i | 3.4 |
| c | 12.5 | j | 3.04 |
| d | 8.5 | k | 1.39 |
| e | 2.4 | l | 1.13 |
| f | 4 | m | 0.44 |
| g | 0.3 | n | 0.15 |

In the antenna design, we are taking two sides of the octagon as the replicated structure. The effective length is two times each side. It describes the initial length in terms of the radius, *r*, of the next nest octagon. An illustration of the process is shown in Figure 1.

The shown structure was replicated three times. Considering the division of the initial segment in two parts; and the initial geometry composed of four segments, the fractal dimension is calculated evaluating (5):

$$h = r\left(\frac{2}{4}\right)^3 = \frac{1}{8}r \tag{6}$$

On the other hand, the effective length is calculated evaluating (4):

$$D = \frac{\log(2)}{\log(4)} = \frac{1}{2} \tag{7}$$

Using fractal structures decreases the resonance frequency, according to (6) and (7) because of the increase of the electrical length. The advantage of the use of fractal structures is that the increase of the electrical length is possible without a significant increase in physical lengths.

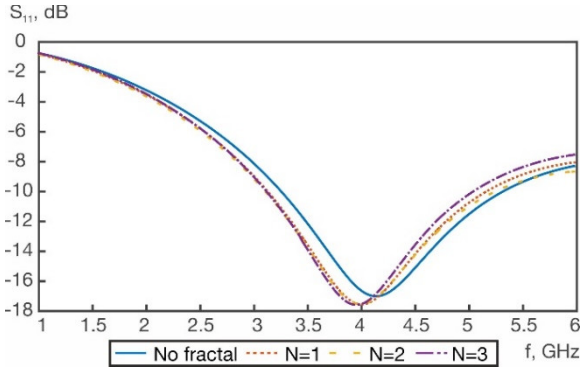


Fig. 3. Simulation of the reflection coefficient of the antenna with N fractal structures.

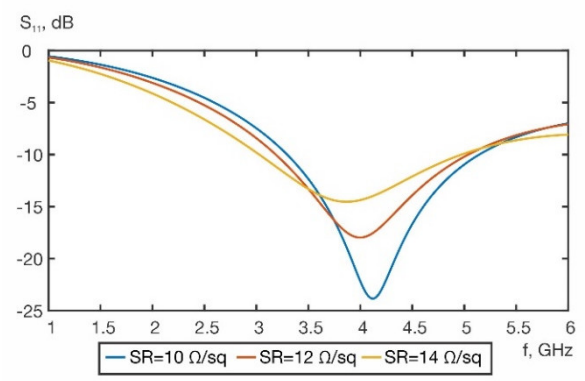


Fig. 4. Simulation of the reflection coefficient of the antenna for different values of sheet resistance.

Then, the proposed fractal antenna is shown in Figure 2. The geometric dimensions of the antenna are represented by the parameters a, b, c, d, e, f, g, h, i, j, k, l, m and n, which values are listed in Table I. The selected substrate is 1.1 mm thick glass, with a relative dielectric permittivity $\varepsilon_r=5$.

The selected conductive film is ITO (Indium-Tin Oxide) whit a thickness of 100 nm (Adafruit Technologies) due to its wide use and its conductive properties. The design of the antenna was made using the software HFSS v13 (Ansys), considering the conductive material as a thin film with a sheet resistance of 10 S/m.

## III. RESULTS

In order to appreciate changes in the reflection coefficient due to the application of the fractal structure, the antenna was simulated for *N* different applied fractal structures. The value for *N=3* was selected, considering it is the maximum value possible due to the tolerances of the fabrication process of the antenna. Figure 3 shows the comparison of the reflection coefficient of the antenna.

A test of the reflection coefficient with different values of sheet resistance was made to demonstrate the impact of the low conductivity film in the bandwidth of the antenna. The results of the test are shown in Figure 4.

Fig. 5. Proposed antenna design.

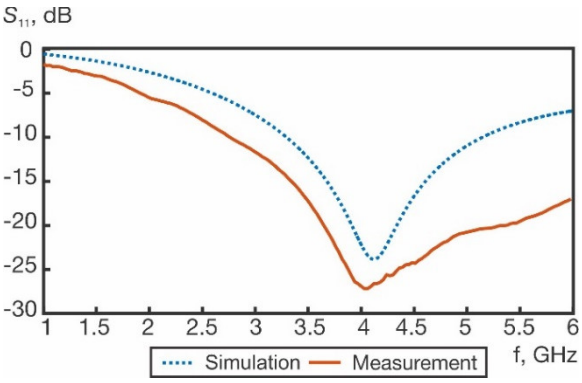


Fig. 6. Simulation and measurement of the reflection coefficient for the antenna.

The final design was obtained after the simulation process. The antenna was fabricated. Figure 5 shows the fabricated antenna. Besides, in Table II, a comparison of respect to the antenna size against other works is presented.

The experimental characterization of the antenna was performed, comparing the results with the data obtained in the simulation. The characterization includes measurements of the reflection coefficient and the gain of the antenna. The measurements of the reflection coefficient were made with a Vector Network Analyzer (VNA) inside a Faraday cage. The connection between the antenna and the VNA was made using an SMA plug, which was soldered with Indium. The union was reinforced with liquid conductive paint. The reflection coefficient $S_{11}$ was measured and compared in Figure 6.

The reflection coefficient $S_{11}$, obtained in measurements, is below -10 dB in the frequency range of 3-6 GHz, with a peak value of -26 dB in the frequency of 4 GHz. In Figure 6, the reflection coefficient $S_{11}$ did no return to -10 dB, as observed in the simulation due to the low conductivity of the ITO film [9], [23].

In order to complete the characterization of the antenna, the radiation pattern, the radiation pattern of total gain was simulated and measured. The measurements of the radiation pattern were made at a frequency of 3.95 GHz. The characterization was made between 0° and 360° in 10° steps.

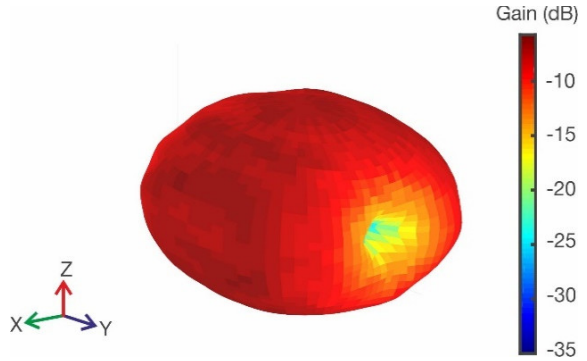


Fig. 7. 3D simulated radiation pattern for the antenna.

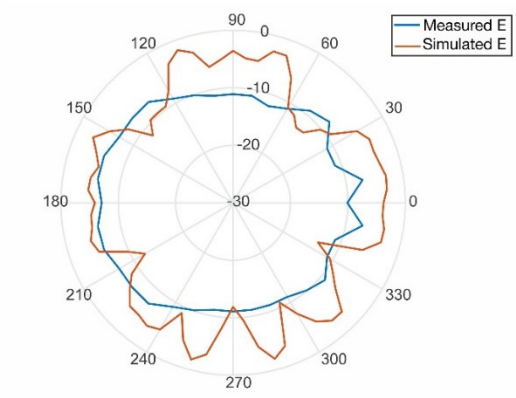


Fig. 8. Simulation and measurement of the radiation pattern for the antenna, E plane.

A 3D radiation pattern is shown in Figure 7. Radiation patterns for the E and H planes are shown in Figures 8 and 9, respectively. The radiation patterns point to an omnidirectional operation, with a peak gain in -6.9 dB. This gain is lower than the typical observed results in wideband planar antennas that use cooper opaque substrates. However, the perceived gain is in concordance to the results observed for other transparent antennas. Moreover, the designed antenna in this work reached the size of the antenna in comparison with other works, which in terms of area, is between 60% [12] and 90% [10] smaller than the antennas proposed by other authors. A comparison of dimensions of the antennas is shown in Table II.

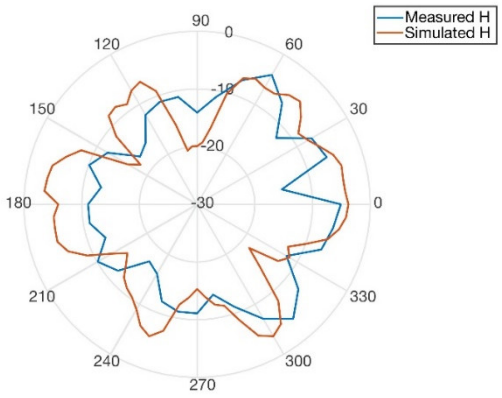


Fig. 9. Simulation and measurement of the radiation pattern for the antenna, H plane.

TABLE II. COMPARISON OF TRANSPARENT ANTENNAS

| Author | Material | Freq. Range (GHz) | $S_{11}$ peak (dB) | Dim. (mm) | Gain (dB) |
|---|---|---|---|---|---|
| [9] | ITO+Au | 2-20 | -20 @7GHz | 45x30 | -4.8 |
| [10] | AZO | 2.4 | -16 @2.4 GHz | 60x50 | ND |
| [11] | $AgHT_4$ | 2.2 | -15 @2.4 GHz | 120x60 | -5 |
| [12] | MMMC | 2.4, 5.8 | -22 @2.4.GHz | 40x20 | -5 |
| [13] | $AgHT_4$ | 2.4, 3.7 | -30 @3.7 GHz | 50x50 | -1.5 |
| This work | ITO | 3-6 | -26 @3.95 GHz | 25x12.5 | -6.9 |

N.D. No data

## IV. CONCLUSIONS

A transparent ITO antenna was presented. The application of a Minkowsky like fractal structure decreases lightly the resonance frequency and improves marginally the reflection coefficient in the desire operation bandwidth. The bandwidth of the antenna is between 3 and 6 GHz, with a peak value in the $S_{11}$ reflection coefficient of -26 dB. The bandwidth of the antenna is longer than the expected and covers all the frequency range for the C-band. The antenna gets a reduction in dimensions in comparison with other transparent antennas without a significative change in the gain. The radiation patterns were measured to show an omnidirectional behavior for the antenna.

## REFERENCES


[1] Huawei, "5G Spectrum," 2016 [Online]. Available: https://www-file.huawei.com/-/media/CORPORATE/PDF/public-policy/public_policy_position_5g_spectrum.pdf

[2] Qualcomm, "Spectrum for 4G and 5G," 2017 [Online]. Available: https://www.qualcomm.com/media/documents/files/spectrum-for-4g-and-5g.pdf

[3] Keysight, "Put Technical Support Front and Center: Pave the Way for a Smooth Migration to 5G," 2020 [Online]. Available: https://www.keysight.com/us/en/assets/7119-1228/white-papers/Put-Technical-Support-Front-and-Center-Pave-the-Way-for-a-Smooth-Migration-to-5G.pdf

[4] FCC, "FCC propuses expanding flexible use of mid-band spectrum," 2018. [Online]. Available: https://docs.fcc.gov/public/attachments/DOC-352520A1.pdf

[5] International Associations of the Satellite Communications Industry, "Position Paper on Interference in C-band by Terrestrial Wireless Applications to Satellite Applications," 2007 [Online]. Available: https://www.itu.int/osg/spu/stn/spectrum/workshop_proceedings/Background_Papers_Final/C-band Interference - Global Position Paper for ITU spectrum workshop.pdf

[6] GSMA, "Use of C-Band spectrum for mobile broadband in cities: London and Shenzhen," 2015 [Online]. Available: https://www.gsma.com/spectrum/wp-content/uploads/2015/10/GSMA_C-Band_Report.pdf

[7] G. Srinivasu, N. Anveshkumar, and V. K. Sharma, "A Compact Octagon Slotted Circular UWB Antenna for RF Energy Harvesting," in *International Conference on Emerging Trends in Information Technology and Engineering, ic-ETITE 2020*, 2020, doi: 10.1109/ic-ETITE47903.2020.383.

[8] S. Kawasaki, S. Yoshida, T. Nakaoka, and K. Nishikawa, "The C-Band HySIC RF Energy Harvester Based on the Space Information, Communication and Energy Harvesting Technology," in *IEEE MTT-S International Microwave Symposium Digest*, 2018, doi: 10.1109/MWSYM.2018.8439367.

[9] S. Hakimi, S. K. A. Rahim, M. Abedian, S. M. Noghabaei, and M. Khalily, "CPW-Fed transparent antenna for extended ultrawideband applications," *IEEE Antennas and Wireless Propagation Letters*, 2014, doi: 10.1109/LAWP.2014.2333091.

[10] M. Awalludin, M. T. Ali, and M. H. Mamat, "Transparent antenna using aluminum doped zinc oxide for wireless application," in *ISCAIE 2015 - 2015 IEEE Symposium on Computer Applications and Industrial Electronics*, 2015, doi: 10.1109/ISCAIE.2015.7298323.

[11] H. J. Song, T. Y. Hsu, D. F. Sievenpiper, H. P. Hsu, J. Schaffner, and E. Yasan, "A method for improving the efficiency of transparent film antennas," *IEEE Antennas and Wireless Propagation Letters*, 2008, doi: 10.1109/LAWP.2008.2008107.

[12] Q. L. Li, S. W. Cheung, D. Wu, and T. I. Yuk, "Optically transparent dual-band MIMO antenna using micro-metal mesh conductive film for WLAN system," *IEEE Antennas and Wireless Propagation Letters*, 2017, doi: 10.1109/LAWP.2016.2614577.

[13] A. Desai, T. Upadhyaya, M. Palandoken, and C. Gocen, "Dual band transparent antenna for wireless MIMO system applications," *Microwave and Optical Technology Letters*, 2019, doi: 10.1002/mop.31825.

[14] J. I. Trujillo-Flores *et al.*, "CPW-Fed Transparent Antenna for Vehicle Communications," *Applied Sciences*, vol. 10, no. 17, p. 6001, Aug. 2020, doi: 10.3390/app10176001. [Online]. Available: https://www.mdpi.com/2076-3417/10/17/6001

[15] C. Balanis, *Antenna Theory: Analysis and Design, Fourth Edition*. 2016.

[16] K. P. Ray, "Design Aspects of Printed Monopole Antennas for Ultra-Wide Band Applications," *International Journal of Antennas and Propagation*, 2008, doi: 10.1155/2008/713858.

[17] A. Katsounaros, Y. Hao, N. Colhngs, and W. A. Crossland, "Optically transparent antenna for ultra wide-band applications," in *European Conference on Antennas and Propagation, EuCAP 2009, Proceedings*, 2009.

[18] Adafruit, "ITO (Indium Tin Oxide) Coated Glass - 50mm x 50mm" [Online]. Available: https://www.adafruit.com/product/1310

[19] R. N. Simons, *Coplanar Waveguide Circuits, Components, and Systems*. 2001.

[20] W. Shu, S. Shichijo, and R. M. Henderson, "A unified equivalent circuit model for coplanar waveguides considering silicon substrate effects," in *IEEE MTT-S International Microwave Symposium Digest*, 2014, doi: 10.1109/MWSYM.2014.6848526.

[21] R. Vivek, G. Yamuna, S. Suganthi, Y. P. Kosta, and M. N. Jivani, "Performance Analysis of Novel Compact Octagonal Shaped Fractal Antenna for Broadband Wireless Applications," *Wireless Personal Communications*, 2018, doi: 10.1007/s11277-018-5511-1.

[22] R. Vivek, G. Yamuna, and S. Suganthi, "Ultra Wideband Octagonal Fractal Antenna using Minkowski geometry for Wireless Applications," *International Journal of Applied Engineer Research.*, vol. 13, pp. 4859–4864, 2018.

[23] T. Yasin, R. Baktur, and C. Furse, "A study on the efficiency of transparent patch antennas designed from conductive oxide films," in *IEEE Antennas and Propagation Society, AP-S International Symposium (Digest)*, 2011, doi: 10.1109/APS.2011.5997183.